Online Automatic Gain Tuning for Geometric Attitude Control

Bee Vang[1] and Roberto Tron[2]

***Abstract*— We present a framework to automatically tune the gains of a geometric attitude controller based on operating conditions (distance from equilibrium). We propose a two-thread architecture: on the one hand, a computationally simple geometric control law provides real-time control inputs to globally stabilize the system; on the other hand, an optimization procedure continuously varies the gains of the control law to improve the convergence rate guarantees when possible. In particular, we use Control Barrier and Lyapunov functions to find rates of change for the gains that improve bounds on the convergence rate while guaranteeing exponential stability for all subsequent times. The advantage of our architecture is that the gain updates can be computed at a rate possibly much slower than the control law; thanks to the constraints used, even if the gain updates were to stop, exponential stability would still be guaranteed for all future times.**

The resulting controller is compared via simulations against a static feedback controller and a version based on traditional discontinuous gain scheduling. While we focus on attitude control, our framework could be generalized to any static feedback controller equipped with explicit convergence conditions.

I. INTRODUCTION

Rigid-body attitude control is an important component of many robotic systems that require particular orientations to collect data or perform meaningful tasks. For instance, quadrotors need to control their attitude in order to change the thrust direction [1]. In aerospace applications, attitude control is used to maneuver or stabilize aircrafts or satellites.

The configuration space of attitudes is non-Euclidean, and traditional control approaches that use a single parametrization (e.g., Euler angles or quaternions [2]) cannot guarantee global stability due to the additional singularities or ambiguities that they introduce. An alternative approach is to develop controllers that take into account the geometry of the underlying differential manifolds ($SO(3)$ for rotations). These geometric controllers [3]–[8] have been shown to exhibit almost global exponential convergence.

Based on these ideas, state-of-the-art hybrid controllers such as [9], [10] partition the state space into regions that are locally stabilized using controllers based on different potential functions [11], [12]. These hybrid controllers achieve global stability by navigating through the different regions with carefully designed switching conditions. However, these approaches are generally more complex and more computationally demanding than simple static feedback controllers, and the switches can produce discontinuous control updates.

This work was supported by the National Science Foundation grant NSF CMMI-1728277.

[1]Department of Mechanical Engineering, Boston University, Boston, MA 02215, USA {bvang@bu.edu}

[2]Department of Mechanical and System Engineering, Boston University, Boston, MA 02215, USA {tron@bu.edu}

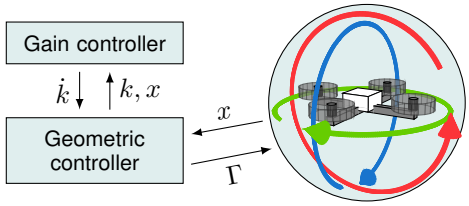

Fig. 1: Our two-thread architecture: A *geometric controller* computes the feedback control input Γ based on the current state x; a *gain controller* updates the gains k of the geometric controller, while ensuring that the each gain update always ensure exponential stability for all subsequent times.

Work in [13], [14] has shown that global stability can be achieved using simple static feedback controllers. Both works are based on time-varying controllers that track an intermediate reference trajectory that, in turn, converges exponentially to a desired equilibrium. The resulting controllers are continuous in time but discontinuous in the initial conditions.

While static feedback controllers are simple to implement and require a very small amount of computation (and thus they can achieve higher control update rates), intuitively, a large convergence basin requires selecting gains that are more conservative in terms of guaranteed convergence rate. In other words, gains that ensure the fastest convergence far from equilibrium might be different those near the equilibrium. The hybrid approach can partially address this problem by partitioning the state space into finer regions at the cost of more complex online switching conditions.

In [15], [16], the authors proposed a method to find a pointwise controller that satisfies safety and stability constraints from Control Barrier and Lyapunov Functions in the form of an optimization problem that can be solved online. As a downside, the existence of a suitable control signal needs to be proved separately; the control is not well-defined when the optimization problem is infeasible. The problem may become infeasible in situations where the system violates safety constraints due to real hardware limitations/noise, or if there is a conflict between safety and stability constraints.

An alternative approach has been presented in [17], where a controller is found by solving an optimization problem based on contraction analysis. The approach ensures global stability by finding a control contraction metric offline, but requires solving path integrals online to find a feedback controller; in general, this is time consuming for systems on manifolds, making the controller unsuitable for fast attitude systems.

At the same time, on the hardware side, it is common to find multicore processors even on an embedded system [18] which allow the execution of multiple computational threads in parallel. In this paper, we take advantage of this opportunity.

Paper contributions. We propose a two-thread architecture (Fig. 1) where a geometric controller computes feedback control inputs at a high update rate, while, in parallel, a gain controller updates its gains at a lower rate. This architecture has the advantage of leveraging the efficient computation and global convergence properties of the geometric controller, while also improving the overall performance guarantees.

For the geometric controller, we use the approach described in [14]. For the gain controller, we propose a point-wise optimization problem with constraints stemming from Control Barrier and Lyapunov Functions, similar to [15]–[17], but we use them to find instantaneous and continuous variations of the gains instead of the control inputs. Thanks to the constraints used in our formulation, even if a feasible solution for the gains update cannot be found, the geometric controller can continue to compute control updates uninterrupted (unlike [15], [16]). Furthermore, we do not require the computation of path integrals despite the use of a time-varying contraction metric (as in [17]).

As a secondary contribution, we derive an extension of Control Barrier Functions to linear matrix inequalities (LMI).

II. Preliminaries and Notation

A. Riemannian Geometry

The work in this paper uses core concepts from Riemannian geometry. A brief overview is provided; for a more in-depth discussion see, e.g., [19]. A rigid body's attitude in three dimensions can be uniquely represented by a rotation matrix $R \in SO(3)$, where $SO(3) = \{R \in \mathbb{R}^{3\times3} : R^T R = I_3, \det(R) = 1\}$. The *tangent space* at a point R on $SO(3)$ is denoted as $T_R SO(3) = \{RV : V \in \mathfrak{so}(3)\}$, where $\mathfrak{so}(3)$ is the set of all 3×3 skew-symmetric matrices. A tangent vector $W \in T_R SO(3)$ can be mapped to a vector $\omega \in \mathbb{R}^3$ using the hat $(\cdot)^\wedge$ and vee $(\cdot)^\vee$ operators:

$$\omega = \begin{bmatrix}\omega_1\\ \omega_2\\ \omega_3\end{bmatrix} \overset{(\cdot)^\wedge}{\underset{(\cdot)^\vee}{\rightleftarrows}} W = R\begin{bmatrix}0 & -w_3 & w_2\\ w_3 & 0 & -w_1\\ -w_2 & w_1 & 0\end{bmatrix}. \quad (1)$$

To simplify the notation, the hat operator at the identity $R = I_3$, is denoted as $\hat{\cdot}$ (i.e., without parentheses). With this notation, $W = (\omega)^\wedge = R\hat{\omega}$ represent the same tangent vector. The *exponential* and *logarithm* maps defined at a rotation R locally transforms tangent vectors into points, and vice versa. The maps are denoted as $\exp_R : T_R SO(3) \to SO(3)$ and $\log_R : U_R \to T_R SO(3)$ where $U_R \subset SO(3)$ is the neighborhood around R for which $\exp_R$ is diffeomorphic. A metric $g : T_R SO(3) \times T_R SO(3) \to \mathbb{R}$ is a family of inner products defined on the tangent space. The notation $g(\cdot,\cdot)_M$ denotes a metric defined by parameters contained in a positive definite matrix M. The covariant derivative $\nabla_X Y$ takes two smooth vector fields X, Y and returns the variation of the field Y along the flow of X.

Second-order rigid body dynamics evolve on the tangent bundle $TSO(3) = \{(R, W) : R \in SO(3), W \in T_R SO(3)\}$, where the state variables are the rotations R and the angular velocities $\omega = W^\vee \in \mathbb{R}^3$ [19]. The *tangent space* at a point (R, W) is denoted as $T_W T_R SO(3) = \{(U, V) : U, V \in T_R SO(3)\}$, and since the tangent space of a tangent space can be identified with itself, tangent vectors in $T_W T_R SO(3)$ can be represented as vertically concatenated matrices using the stack function, e.g. $\mathrm{stack}(U, V) = \left[\begin{smallmatrix}U\\V\end{smallmatrix}\right]$.

B. Rigid Body Dynamics

Rigid body rotations can be modeled as a simple mechanical system evolving on $TSO(3)$. The general dynamical equations on a manifold $\mathfrak{M}$ are [19]

$$\nabla_{\dot{x}}\dot{x} = J^{-1}(-dP(x) + \sum_{i=1}^{m} F_i(x, \dot{x})u_i), \quad (2)$$

where $x \in \mathfrak{M}$, $(x, \dot{x}) \in T\mathfrak{M}$, J is the inertia matrix, $P : \mathfrak{M} \to \mathbb{R}$ is a smooth function describing the potential energy, dP represents the differential of P, F_i is a collection of one forms representing the external forces on the system, and $u_i \in \mathbb{R}$ is the control input. In particular, the equations of motion for rigid body attitudes are

$$\dot{R} = R\hat{\omega}, \quad \dot{\omega} = \Gamma - J^{-1}\left(\omega \times J\omega\right), \quad (3)$$

where $R \in SO(3)$ is a rotation from body to inertial frame, $\omega \in \mathbb{R}^3$ is the angular velocity, $J \in \mathbb{R}^{3\times3}$, and $\Gamma \in \mathbb{R}^3$ is the moment vector (control input), all expressed in body frame.

C. Contraction Theory

Contraction theory [20], [21] is used to show stability of a system by studying the behavior of nearby trajectories. If infinitesimally neighboring trajectories converge, i.e., if the virtual displacements δ_x (vector fields, in differential geometry terminology) between them converge to zero, then the system is stable, leading to the following result.

Proposition 1 (Adapted from [21]): A system $\dot{x} = f(x)$ evolving on a manifold is contracting with guaranteed exponential convergence rate β if there exist a metric g defined by parameters in matrix a M, and with the corresponding Levi-Civita connection ∇, such that, for any vector field δ_x,

$$g\left(\nabla_{\delta_x} f, \delta_x\right)_M \leq -\beta g\left(\delta_x, \delta_x\right)_M. \quad (4)$$

D. Geometric Control Lyapunov Functions

Control Lyapunov functions (CLF) are used to synthesize stabilizing feedback controllers by solving point-wise optimization problems. In the case of this paper, CLFs are used to achieve desired objectives (when possible) that can be described by potential functions.

Proposition 2 (Adapted from [16]): For a simple mechanical system (2), a continuously differentiable function $V : T\mathfrak{M} \to \mathbb{R}$ is a Control Lyapunov Function (CLF) if there exist constants $c_1, c_2 > 0$ such that,

$$V(x, \dot{x}) \geq c_1(\Psi(x, x_d) + g\left(X(\dot{x}, \dot{x}_d), X(\dot{x}, \dot{x}_d)\right)), \quad (5)$$

$$V(x, \dot{x}) \leq c_2(\Psi(x, x_d) + g\left(X(\dot{x}, \dot{x}_d), X(\dot{x}, \dot{x}_d)\right)), \quad (6)$$

$$\inf_{u\in\mathbb{R}^m}\{\langle d_1 V, \dot{x}\rangle - \langle d_2 V, J^{-1}dP\rangle + \sum_{i=1}^{m}\langle d_2 V, J^{-1}F_i\rangle u_i\} \leq 0, \quad (7)$$

for all $(x, \dot{x}) \in T\mathfrak{M}$, where $\Psi(x, x_d)$ is an error function between $x, x_d \in \mathfrak{M}$, $X(\dot{x}, \dot{x}_d) \in T_x\mathfrak{M}$ is a tangent vector representing the velocity error from $\dot{x}$ to $\dot{x}_d$, $d_i V$ is the differential of V with respect to the i-th argument, and $\langle d_i V, Y\rangle$ is the value of the one-form $d_i V$ applied to the vector field Y.

E. Geometric Zeroing Control Barrier Functions

Zeroing Control Barrier functions (ZCBF) are similar to CLFs, but are used to ensure that a set is *forward-invariant*. A set $\mathcal{S}$ is called forward-invariant if, for every $x_0 \in \mathcal{S}$, $x(t, x_0) \in \mathcal{S}$ for all time t.

Proposition 3 (Adapted from [15], [16]): Given a smooth function $h : T\mathfrak{M} \to \mathbb{R}$ and a safety set defined by $\mathcal{C} = \{(x, \dot{x}) \in T\mathfrak{M} : h(x, \dot{x}) \geq 0\}$; the function h is a Zeroing Control Barrier Function (ZCBF) if there exist an extended class $\mathcal{K}$ function α such that,

$$\inf_{u \in \mathbb{R}^m} \{\langle d_1 h, \dot{x} \rangle - \langle d_2 h, J^{-1} dP \rangle + \sum_{i=1}^{m} \langle d_2 h, J^{-1} F_i \rangle u_i + \alpha(h)\} \geq 0 \quad (8)$$

for all $(x, \dot{x}) \in \mathcal{C}$. A function $\alpha : (-b, a) \to (-\infty, \infty)$ for some $a, b > 0$ is said to be extended class $\mathcal{K}$ if it is strictly increasing and $\alpha(0) = 0$.

F. Geometric Controller with Exponential Global Convergence

In this section we review the geometric controller from [14]. However, our gain controller could be applied in tandem with other controllers whenever explicit stability conditions are available (such as [6]). The geometric PD attitude controller in [14] achieves global exponentially stability by introducing a time-varying reference trajectory R_{ref} that augments the system dynamic equations (3) with

$$\dot{R}_{ref} = -k_{ref} R_{ref} \hat{e}_{R_{ref}}, \quad (9)$$

and the controller

$$\Gamma = J^{-1}(\omega \times J\omega) - k_d e_R - k_v e_\omega, \quad (10)$$

where k_d, k_v, k_{ref} are positive feedback gains. The dynamics of the augmented system lives on the product manifold $TSO(3) \times SO(3)$. The error terms, e_R, $e_{R_{ref}}$, and e_ω are derived from two configuration error functions $\Psi_R(R, R_{ref}), \Psi_{R_{ref}}(R_{ref}, R_d)$ on $SO(3)$ where R_d is the desired attitude. Then, the error terms for the controller and reference trajectory are (with $r \in \{R, R_{ref}\}$)

$$e_{r \in \{R, R_{ref}\}} = (\mathrm{grad}_1(\Psi_r))^\vee, \quad e_\omega = \omega - \omega_d = \omega, \quad (11)$$

where grad_i is the gradient with respect to the i-th argument, and, without loss of generality, $\omega_d = 0$. Note that by selecting $k_{ref} = 0$ and $R_{ref} = R_d$ (i.e. setting the reference trajectory to the desired attitude), we recover the controller of [22] as a particular case.

Global stability is proved by applying the contraction condition (4) with the Riemannian metric,

$$g(X, Y)_M = \frac{1}{2} \mathrm{tr}\left(X^T (M \otimes I_3) Y\right) \quad (12)$$

for all $R \in SO(3)$ where X, Y are tangent vectors on $TSO(3) \times SO(3)$,

$$M = \begin{bmatrix} m_1 & m_2 & m_6 \\ m_2 & m_3 & m_5 \\ m_6 & m_5 & m_4 \end{bmatrix} \in \mathbb{S}^n_+, \quad m_{i \in \{1,\ldots,6\}} \in \mathbb{R}, \quad (13)$$

$\mathbb{S}^n_+$ denotes the set of all positive definite matrices, and $\otimes$ is the Kronecker product. Note that matrix inequalities in this paper refers to positive (semi-)definite matrices.

The work in [14] identified bounds $\mathcal{D}_j \leq 0$ that imply the contraction condition (4) using the metric 12, where

$$\mathcal{D}_1 = -m_2 k_d \min\Big(\mathrm{dg}\big(\mathrm{Re}(\Lambda_R)\big)\Big) + \mathcal{B}_{2,1} + \mathcal{B}_{3,1} + \sqrt{3} \max\left|\frac{1}{4} m_2' \|\omega\|^2 \begin{bmatrix} 0 \\ -1 \end{bmatrix} + m_1 \beta\right|, \quad (14)$$

$$\mathcal{D}_2 = m_2 - m_3 k_v + m_3 \beta + \mathcal{B}_{2,1} + \mathcal{B}_{3,2}, \quad (15)$$

$$\mathcal{D}_3 = -m_4 k_{ref} \min\Big(\mathrm{dg}\big(\mathrm{Re}(\Lambda_{R_{ref}})\big)\Big) + \mathcal{B}_{3,1} + \mathcal{B}_{3,2} + \sqrt{3} \max\left|m_5 k_d \mathrm{dg}\big(\mathrm{Re}(\Lambda_R)\big) + m_4 \beta I_3\right|, \quad (16)$$

where

$$\mathcal{B}_{2,1} = \sqrt{3}\left|-\frac{1}{8} m_3' \|\omega\|^2\right| + \sqrt{3}\left|-\frac{1}{4}\left(m_2' - m_3' k_v\right)\|\omega\|\right| + \sqrt{3} \max\left|\frac{(m_1 - m_2 k_v + 2\beta m_2) - m_3 k_d \mathrm{dg}(\Lambda_R)}{2}\right| + \sqrt{3}\left|\frac{k_d}{4} m_3' \theta_R\right|,$$

$$\mathcal{B}_{3,1} = \sqrt{3} \max\left|\frac{k_d}{2}\left(m_2 - m_5\right)\mathrm{dg}(\Lambda_R)\right| + \sqrt{3}\left|\frac{m_5 m_6 k_d}{4 m_4} \theta_R\right| + \sqrt{3}\left|\frac{m_6^2 - m_5 m_6 k_v}{4 m_4}\|\omega\|\right| + \sqrt{3}\left|\frac{m_6 k_{ref}}{4} \theta_{R_{ref}}\right| + \sqrt{3} \max\left|-\frac{m_6 k_{ref}}{2} \mathrm{dg}\big(\Lambda_{R_{ref}}\big) + m_6 \beta\right|,$$

$$\mathcal{B}_{3,2} = \sqrt{3} \max\left|\frac{m_3 k_d}{2} \mathrm{dg}\big(\Lambda_R\big) + \frac{1}{2}\left(m_6 - m_5 k_v\right)\right| + \max\left|-\frac{m_5 k_{ref}}{2} \mathrm{dg}\big(\Lambda_{R_{ref}}\big) + m_5 \beta\right| + \sqrt{3}\left|\frac{m_5^2 k_d}{4 m_4} \theta_R\right| + \sqrt{3}\left|\frac{m_5 m_6 - m_5^2 k_v}{4 m_4}\|\omega\|\right| + \sqrt{3}\left|\frac{m_5 k_{ref}}{4} \theta_{R_{ref}}\right|,$$

$$m_2' = m_2 - \frac{m_5 m_6}{m_4}, \quad m_3' = m_3 - \frac{m_5^2}{m_4}.$$

The parameters $\|\omega\|$, θ_R, and $\theta_{R_{ref}}$ are the norms of ω, e_R, and $e_{R_{ref}}$ while $\Lambda_R, \Lambda_{R_{ref}}$ are the eigenvalue matrix of the differentials of e_R and $e_{R_{ref}}$, respectively. The operator $\mathrm{dg}(\cdot)$ extracts the diagonal elements of a matrix as a vector or the inverse for a vector argument and $\mathrm{Re}(\cdot)$ extracts the real part of the argument.

We can expand each of the above conditions by replacing each $\max$ function with one of its γ_i arguments where i is the i-th $\max$ function for the given condition (e.g. $\mathcal{D}_1$ has $i = \{1, 2, 3, 4\}$) resulting in $\prod_i \gamma_i$ bounds. The product results from taking into account all the possible combinations of all terms within all the $\max$ functions. Furthermore, each absolute value term can be expanded into two bounds by replacing them with the positive or negative argument. For each condition with $\rho_k \geq 0$ absolute value terms, there are 2^{ρ_k} bounds. Taken together, expanding $\mathcal{D}_1, \mathcal{D}_2$, and $\mathcal{D}_3$ results (with a slight abuse of notation) in the constraints $\mathcal{D}_j \leq 0$, where $j \in \{1, \ldots, \sum_1^3 2^{\rho_k} \prod_i \gamma_i\}$ (the expanded constraints contain the same terms as above, but with different signs).

In [14], the authors used conservative bounds for $\|\omega\|$, θ_R, and $\theta_{R_{ref}}$, and used offline optimization to find values for the matrix M, the gains k_d, k_v, k_{ref} and the guaranteed convergence rate β that satisfy all the constraints. It was

empirically noticed [22, Table III] that smaller bounds on the states would result in better values for the convergence rate.

III. Constraints for the gain controller

Following the above observation, since the guaranteed convergence rate depends on the bounds on the angular speed and angles, we propose to vary the gains k_d, k_v, k_{ref} based on the current state, to improve the convergence rate guarantees as the system moves toward the equilibrium. Ideally, one could repeat the offline optimization described in [14] for different bounds, and build a look-up table mapping each state x to a set of gains; this approach, however, is computationally infeasible, and could result in discontinuous gains and thus discontinuous control signals. Instead, we propose to apply dynamic extension (Sec. III-A) and find updates $\dot{k}_d, \dot{k}_v, \dot{k}_{ref}, \dot{\beta}$ for the gains and estimated convergence rate that *1)* still satisfy all the previous stability conditions (Sec. III-B to III-D), *2)* guaranteed bounded control signals (Sec III-E), and *3)* aim to improve a weighted combination of control effort and guaranteed convergence rate (Sec. III-F). All these constraints and objective function are then combined in a gain controller (as described in Sec. IV).

A. Dynamic Extension

In order to improve the smoothness of the control signals, and also ensure satisfaction of all the constraints on the gains in a way that is amenable for real-time computations, we use the concept of *dynamic extension*. The goal is not to directly find new parameters, but instead control their derivatives via point-wise updates. In practice, we make the gains, metric parameters, and convergence rate become part of the state of the close-loop system, and evolve them by specifying their derivatives $\dot{k}_d, \dot{k}_v, \dot{k}_{ref}$, $\dot{m}_{i\in\{1,\dots,6\}}$, and $\dot{\beta}$. Accordingly, the state space becomes

$$x = (R, \omega, R_{ref}, k_d, k_v, k_{ref}, m_i, \beta), \tag{17}$$

and the control (i.e., the eventual optimization variable) is

$$u = \text{stack}(\dot{k}_d, \dot{k}_v, \dot{k}_{ref}, \dot{m}_i, \dot{\beta}). \tag{18}$$

Remark 1: In traditional contraction analysis, the matrix M can be defined via functions that depend on the state (or found online by solving path integrals as in [17]), making it time varying, and thus introducing an additional term in (4). Then, in general, it becomes difficult to use this principle to ensure stability. However, with the dynamic extension above, we directly control the rate of change of the metric, and the aforementioned issue is avoided.

B. Stability Constraints

The dynamic extension of the system allows us to leverage the stability results of the underlying fixed gain controller. From Sec. II-F, if the constraints $\mathcal{D}_j \leq 0$ are satisfied for a state then convergence is guaranteed starting at that state. We therefore propose to use the constraints as ZCBFs

$$h_{conv,j} = -\mathcal{D}_j \geq 0 \tag{19}$$

to ensure that the controller is always stable. The resulting stability constraints are

$$\begin{aligned}\left\langle d_{(R,\omega,R_{ref})} h_{conv,j}, (\dot{R}, \dot{\omega}, \dot{R}_{ref}) \right\rangle \\ + \left\langle d_{(k_d,k_v,k_{ref},m_i,\beta)}, (\dot{k}_d, \dot{k}_v, \dot{k}_{ref}, \dot{m}_i, \dot{\beta}) \right\rangle \\ + \alpha_{conv,j}(h_{conv,j}) \geq 0\end{aligned} \tag{20}$$

where we use the notation $\left\langle d_{(a,b)} h, (\dot{a}, \dot{b}) \right\rangle = \langle d_a h, \dot{a} \rangle + \left\langle d_b h, \dot{b} \right\rangle$ as a shorthand expression for sums of one-forms.

Remark 2: The constraints $\mathcal{D}_j \leq 0$ are conservative and in fact stability is still guaranteed if the exact contraction condition (4) is met (see [14, Remark 10]). In principle, one could instead apply (4) directly; however, the results would then hold only for that time instant. Instead, since the bounds from Sec. II-F are obtained by considering an entire convergence basin around the equilibrium, the results from [14] can be used to guarantee contraction, and hence exponential stability, for all subsequent times (even if the gains were to be kept constant from that moment on).

Remark 3: Since the bounds $\mathcal{D}_j$ are homogeneous in m_i, the constraint $m_4 = 1$ is added to improve numerical stability (see also [14, Remark 11]).

C. Convergence Rate Bound Constraint

The contraction condition (4) ensures exponential convergence only when the convergence rate bound is greater than zero, i.e. $\beta > 0$. This constraint is enforced using the ZCBF

$$h_\beta = \beta - \beta_{\min} \geq 0 \tag{21}$$

for some lower bound $\beta_{\min}$. The resulting convergence rate bound constraint is

$$\dot{\beta} + \alpha_\beta(\beta - \beta_{\min}) \geq 0. \tag{22}$$

Remark 4: In practice, $\beta_{\min}$ is set to a small number just greater than 0 to prevent $\beta \to 0$. Note that β is a lower bound, thus the system can achieve faster convergence rates.

D. Metric Constraint

The stability constraints from Sec. III-B allows the metric parameters m_i to change in any manner. While this does not have a physical impact on the controller or real system behavior, the new parameters must form a positive definite matrix to ensure that (12) is a proper Riemannian metric. This can be achieved by extending ZCBFs from scalar functions to linear matrix inequalities (LMI) as shown in the following novel proposition.

Proposition 4: Let $\mathbb{S}_\epsilon$ be the set of positive definite matrices such that $M \geq \epsilon I$ for some constant $\epsilon > 0$ and the identity matrix I. Then the condition with arbitrary $c_m \geq 0$,

$$\dot{M} + c_m M \geq \epsilon I, \tag{23}$$

makes the set of positive definite matrices $\mathbb{S}_\epsilon$ forward-invariant for M, i.e. $M(0) \in \mathbb{S}_\epsilon$ implies $M(t) \in \mathbb{S}_\epsilon$ for all $t > 0$.

Proof: The condition $M \geq \epsilon I$ is equivalent to requiring

$$h_{m,X}(M) = \frac{1}{2} \operatorname{tr}\left(X^T (M \otimes I_3) X\right) - \epsilon I \geq 0 \tag{24}$$

for all tangent vectors $X \neq 0$. We can interpret $h_{m,X}$ as a scalar ZCBF indexed by X, i.e. we have an infinite number of constraints associated with an infinite number of ZCBFs, and we have that $\mathbb{S}_\epsilon = \cap_{X \neq 0} \{M : h_{m,X}(M) \geq 0\}$. The corresponding CBF constraint with a linear class $\mathcal{K}$ function,

$$\frac{1}{2} \operatorname{tr}\left(X^T (\dot{M} \otimes I_3) X\right) + c_m \frac{1}{2} \operatorname{tr}\left(X^T (M \otimes I_3) X\right) \geq \epsilon I,$$

$$\frac{1}{2}\operatorname{tr}\left(X^T((\dot{M}+c_mM)\otimes I_3)X\right)-\epsilon I\geq 0, \tag{25}$$

makes the set $\{M : h_{m,X}(M) \geq 0\}$ forward-invariant. It follows that the intersection of all the constraints (25) makes $\mathbb{S}_\epsilon$ forward-invariant. Lastly, such intersection is equivalent to the constraint in the claim. ■

E. Gain Constraints

Real systems have control limitations such as minimum and maximum torques. Typically, these limitations are represented as a constraint on the control, i.e. $\tau_{\min} \leq \Gamma \leq \tau_{\max}$. However, the optimization variables here correspond to the rate of change of the control so the standard constraint cannot be used. Instead, we indirectly ensure that the control is bounded by bounding the gains k_d, k_v. Also the k_{ref} gain is bounded in the same manner for numerical stability especially when $R_{ref} \approx R_d$. We upper and lower bound the $\ell \in \{d, v, ref\}$ indexed gain, k_ℓ, with $k_{\ell,\max}, k_{\ell,\min}$, respectively, using the following ZCBFs

$$h_{k_\ell,\max} = k_{\ell,\max} - k_\ell \geq 0, \tag{26}$$

$$h_{k_\ell,\min} = k_\ell - k_{\ell,\min} \geq 0. \tag{27}$$

The resulting gain constraints are

$$-\dot{k}_\ell + \alpha_{k_\ell,\max}(k_{\ell,\max} - k_\ell) \geq 0 \tag{28}$$

$$\dot{k}_\ell + \alpha_{k_\ell,\min}(k_\ell - k_{\ell,\min}) \geq 0. \tag{29}$$

Remark 5: the constraint $\tau_{\min} \leq \Gamma \leq \tau_{\max}$ may be enforced directly as two ZCBFs. This will be explored in future works.

F. Objective Function

A benefit of point-wise optimization is that an objective function can be specified for the current state. A desirable objective is to reduce the overall energy consumption, i.e. $\min \int \|\Gamma\|^2$. However, as in Sec. III-E, the control effort cannot be directly constrained. Instead we propose the CLF

$$V_\Gamma = \|\Gamma\|^2 \tag{30}$$

with a slack variable δ resulting in constraint

$$\left\langle d_{(k_d,k_v,k_{ref},m_i,\beta)}V_\Gamma, (\dot{k}_d,\dot{k}_v,\dot{k}_{ref},\dot{m}_i,\dot{\beta})\right\rangle + \left\langle d_{(R,\omega,R_{ref})}V_\Gamma, (\dot{R},\dot{\omega},\dot{R}_{ref})\right\rangle \leq \delta. \tag{31}$$

The slack variable δ ensures that constraint (31) can always be satisfied. In other words, reducing the control effort is not a primary objective and should only be achieved when all other more important constraints are satisfied.

By transforming the above objective into a constraint, a more general quadratic cost function can be utilized

$$\min_{u=\text{stack}(\dot{k}_d,\dot{k}_v,\dot{k}_{ref},\dot{m}_i,\dot{\beta},\delta)} \quad u^TQu + P^Tu. \tag{32}$$

for some weighting matrices $Q \geq 0, P \in \mathbb{R}^{11}$.

IV. Attitude Controllers

Our proposed varying-gains attitude controller is presented in this section along with two other similar controllers (all based on (10)) for comparison.

A. Static Controller (Time-Varying, [14])

The baseline attitude controller is the static controller (SC) from [14] using static gains, metric parameters, and convergence rate. In particular, the cost functions $\Psi_R, \Psi_{R_{ref}}$ are chosen to be (with $r \in \{R, R_{ref}\}$),

$$\Psi_{r\in\{R,R_{ref}\}}(R_1,R_2) = \frac{1}{2}\|(\log_{R_1} R_2)^\vee\|^2 \tag{33}$$

with gradient [23, Prop. 2.2.1],

$$\operatorname{grad}_1(\Psi_r) = -\log_{R_1} R_2. \tag{34}$$

Note that $\theta_r = \|(\log_{R_1} R_2)^\vee\|$.

The best static gains, metric parameters, and convergence rate are determined via the algorithm found in [14, Algorithm 1]. The algorithm requires user-selected maximum initial parameters $\theta_{R,\max}, \theta_{R_{ref},\max}$, and $\|\omega\|_{\max}$ which define a contraction region on the state space defined by the initial distance between R and R_{ref}, R_{ref} and R_d, and the initial speed, respectively. The sum $\theta_{R,\max} + \theta_{R_{ref},\max}$ represents the maximum initial distance that R can be away from R_d such that convergence holds by contraction theory. For the cost function (33), the maximum $\theta_r(r, R_d)$ is π [23]; therefore the sum must be chosen to be greater than or equal to π to ensure global stability. Lastly, the algorithm requires a list of initial desired gains. From [22], we have an idea of the optimal k_d, k_v gains, therefore we only need to do a search over the k_{ref} gain. The chosen values and resulting best gains and convergence rate are shown in Table I. The corresponding metric parameters are

$$M = \begin{bmatrix} 0.0347 & 0.0003 & 0.0140 \\ 0.0003 & 0.0001 & 0.0003 \\ 0.0140 & 0.0003 & 1.000 \end{bmatrix}. \tag{35}$$

TABLE I: Static Controller Parameters

Parameter	Value	Description
J	$\operatorname{dg}(\text{stack}(5,2,1))$	Inertia matrix
k_d	100	Initial rotation error gains
k_v	80	Initial velocity error gains
k_{ref}	$[1, 5, 10, ..., 100]$	Initial reference trajectory gains
$\|\omega\|_{\max}$	1	Max initial angular speed
$\theta_{R,\max}$	$\pi/4$	Max init. dist. error R to R_{ref}
$\theta_{R_{ref},\max}$	$3\pi/4$	Max init. dist. error R_{ref} to R_d
β^*	0.4022	Best guaranteed convergence rate
k_d^*	106.6667	Best rotation error gain
k_v^*	74.6667	Best angular velocity error gain
k_{ref}^*	0.9833	Best reference trajectory gain

B. Varying-Gains Controller (This Paper)

The varying-gains controller (VGC) utilizes a semi-definite program (SDP) to update the gains along the trajectory. The optimization problem select gains such that the contraction conditions hold at every time instant with bounds given by the current state (R, ω, R_{ref}). Intuitively, the aim is to change the gains toward the optimal ones that we would obtain by repeatedly applying the previous approach [14] while setting $\theta_{R,\max} = \theta_R(R, R_{ref})$, $\theta_{R_{ref},\max} = \theta_{R_{ref}}(R_{ref}, R_d)$, and $\|\omega\|_{\max} = \|\omega\|$.

Theorem 1: Given initial states and parameters $(R_0, \omega_0, R_{ref,0}, k_{d,0}, k_{v,0}, k_{ref,0}, m_{i,0}, \beta_0)$ that satisfies (4)

for system (9) with controller (10), the close-loop system is (globally) stable with dynamic gains, metric parameters, and convergence rate when they are updated according to the solution of the point-wise SDP below. If the problem is infeasible, then set $u = \text{stack}(0, 0, 0, 0, 0, 0)$ and stability is still maintained. The SDP is

$$\begin{aligned} \min_{u=\text{stack}(\dot{k}_d, \dot{k}_v, \dot{k}_{ref}, \dot{m}_i, \dot{\beta}, \delta)} \quad & u^T Q u + P^T u \\ \text{s.t.} \quad & (20) \quad \text{(Stability CBF)} \\ & (22) \quad (\beta \text{ L.B. CBF}) \\ & (23) \quad \text{(Metric CBF)} \\ & (31) \quad (\|\Gamma\|^2 \text{ CLF}) \\ & (28) \quad \text{(Gain U.B. CBF)} \\ & (29) \quad \text{(Gain L.B. CBF)} \\ & c_{k_{\ell,L.B.}} \leq \dot{k}_\ell \leq c_{k_{\ell,U.B}} \end{aligned} \tag{36}$$

where $c_{k_{\ell,L.B.}}, c_{k_{\ell,U.B}} \in \mathbb{R}$ are constants.

Proof: If the SDP (36) is feasible, then the gains, metric parameters, and convergence rate can instantaneously update according to the solution $u = \text{stack}(\dot{k}_d, \dot{k}_v, \dot{k}_{ref}, \dot{m}_i, \dot{\beta})$. Furthermore, (20) is a ZCBF guaranteeing that the contraction bounds (14)–(16) will remain negative, thus proving stability by contraction theory. If the SDP is infeasible, then setting $u = 0$ means that the gains, metric parameters, and convergence rate are unchanged. Then, by the last feasible solution and state (or initial condition), the states still converge exponentially [14, Theorem 1]. ■

Proposition 5: The control signal Γ produced by the gain controller above is Lipschitz continuous.

Proof: The varying-gains controller is composed of continuous functions, and the gains are Lipschitz continuous by $c_{k_{\ell,L.B.}} \leq \dot{k}_\ell \leq c_{k_{\ell,U.B}}$. Hence, the control signal Γ is also Lipschitz continuous [15, Fact 2]. ■

Remark 6: Although there are many constraints, they are all linear and only a few are active at any time which means that they can be solved quickly. In particular, the optimization problem (36) with parameters from Table II averages $0.2428s$ to solve with CVX [24] using the SDPT3 solver [25] in MATLAB. Faster results could be obtained with specialized implementations on real systems.

Remark 7: Our approach allows the gains to remain constant at any point and the system would still converge. This has the advantage that if the optimization (36) becomes infeasible, we can keep the same gains between updates. As a result, the actual control law (10) for Γ can be computed at a much higher rate (see Fig. 1).

To be consistent with the static controller (SC), the initial gains, metric parameters, and convergence rate are set to the same values. The constraints in (36) require class $\mathcal{K}$ functions. For simplicity, we choose a linear class $\mathcal{K}$ function for all. Lastly, a particular cost function is defined for the simulations. We choose a linear combination of improving convergence rate (increasing $\dot{\beta}$) and reducing control effort (decreasing δ). The experimentally chosen parameters for the varying-gains controller is given in Table II.

TABLE II: Varying-Gains Controller Parameters

Parameter	Value	Description
$k_{d,0}$	106.6667	Init. rotation error gain
$k_{v,0}$	74.6667	Init. velocity error gain
$k_{ref,0}$	0.9833	Init. ref. trajectory gain
c_{conv}	1	Convergence CBF factor
$\beta_{\min}$	1^{-6}	Min convergence rate
c_m	1	Metric CBF factor
$k_{\ell,\max}$	110	Max gain
$k_{\ell,\min}$	0	Min gain
Q	0	Quadratic cost matrix
P	$\text{stack}(0, 0, 0, 0_i, -c_\beta, c_\delta)$	Linear cost matrix
c_β	10	Convergence weight
c_δ	1	Minimize control weight

TABLE III: Gain Schedule Constants

Parameter	Value	Description
k_d	$[0.1, 10, 20, ..., 110]$	Initial rotation error gains
k_v	$[0.1, 10, 20, ..., 110]$	Initial velocity error gains
k_{ref}	$[0.1, 5, 10]$	Initial reference trajectory gains
$\|\omega\|_{\max}$	1	Max initial angular speed

C. Gain Schedule Controller (Baseline)

A straightforward approach to improve a static controller is to gain schedule for different convergence regions. The gain schedule controller (GSC) uses the same controller as the SC, but the gains are changed to some optimal ones when the system is within specified convergence regions. The gains for each region are computed offline using [14] for different values of $\theta_{R,\max}, \theta_{R_{ref},\max}$, and $\|\omega\|_{\max}$.

For comparison, the state space is split into four regions by distance to the desired attitude. The constant parameters and gains search space for each region is given in Table III. The regions and resulting best gains are given in Table IV.

During run-time, the control gains are updated when the distance between the current R and desired R_d attitudes first reach an initial distance as defined by $\theta_{R,\max} + \theta_{R_{ref},\max}$ and the contraction condition (4) is satisfied with the new convergence region parameters and current state (see Remark 2). If the current state (R, ω, R_{ref}) does not satisfy the contraction condition then the reference trajectory is updated to $R_{ref} = \exp_R(\theta_{R,\max} \frac{\omega}{\|\omega\|})$ (an attitude that is $\theta_{R,\max}$ distance away from R in the direction of ω) or $R_{ref} = R_d$ (local controller [22]). If the modified state still does not satisfy the contraction condition, no gain update is made (to maintain stability) and the process is repeated.

Remark 8: The reference trajectory R_{ref} can be arbitrary chosen because it is fictitious. The updated reference attitude is chosen such that the bounds (14)–(16) are satisfied by the θ_R and $\theta_{R_{ref}}$ parameters. However, the contraction metric can still be violated due to the angular velocity ω. In our case, we switch to the local controller after leaving the global region.

V. Results and Simulation

In this section, we compare the attitude controllers of the previous section. The initial condition for all the simulations are chosen to be the same and far away from the identity so that a global controller is required. All three controllers start with initial gains and parameters from Table I. The desired state is $(R_d = I_3, \omega_d = 0) \in TSO(3)$. The initial states are

TABLE IV: Gain Schedule Regions

Parameter	Value	Description
Global Region		
$\theta_{R,\max}$	$\pi/4$	Max init. dist. error R to R_{ref}
$\theta_{R_{ref},\max}$	$3\pi/4$	Max init. dist. error R_{ref} to R_d
β^*	0.4022	Best convergence bound
k_d^*	106.6667	Best rotation error gain
k_v^*	74.6667	Best velocity error gain
k_{ref}^*	0.9833	Best reference trajectory gain
$3\pi/4$ **Region**		
$\theta_{R,\max}$	$3\pi/4$	Max init. dist. error R to R_{ref}
$\theta_{R_{ref},\max}$	0	Max init. dist. error R_{ref} to R_d
β^*	1.4296	Best convergence bound
k_d^*	110	Best rotation error gain
k_v^*	30.1000	Best velocity error gain
k_{ref}^*	0	Best reference trajectory gain
$\pi/2$ **Region**		
$\theta_{R,\max}$	$\pi/2$	Max init. dist. error R to R_{ref}
$\theta_{R_{ref},\max}$	0	Max init. dist. error R_{ref} to R_d
β^*	3.3329	Best convergence bound
k_d^*	110	Best rotation error gain
k_v^*	22.1100	Best velocity error gain
k_{ref}^*	0	Best reference trajectory gain
$\pi/4$ **Region**		
$\theta_{R,\max}$	$\pi/4$	Max init. dist. error R to R_{ref}
$\theta_{R_{ref},\max}$	0	Max init. dist. error R_{ref} to R_d
β^*	5.4195	Best convergence bound
k_d^*	110	Best velocity error gain
k_v^*	20.1000	Best velocity error gain
k_{ref}^*	0	Best reference trajectory gain

chosen such that R_0 is the maximum distance π away from the identity, $R_{ref,0}$ is randomly chosen to be $\theta_{R_{ref},\max} = 3\pi/4$ away from the identity and $\theta_{R,\max} = \pi/4$ from R_0, and $\omega_0 = \frac{\left(\log_{R_0} R_{ref,0}\right)^\vee}{\|\left(\log_{R_0} R_{ref,0}\right)^\vee\|}$ (moving towards $R_{ref,0}$ at unit speed).

Figure 2 depicts the distance and speed error of the controllers. The SC and VGC have similar smooth behavior as they converge. The VGC seems to converge faster both in distance and speed. The GSC experiences an abrupt change during the first gain switching phase at $0.57s$, then continues to converge rapidly with high speeds.

To prove convergence, the maximum eigenvalue of the contraction matrix (derived from the contraction condition (4) as shown in [14], [22]) is shown in Figure 3. As expected, all controllers maintain a negative maximum eigenvalue ensuring exponential stability by satisfying the contraction condition (4). The system is considered to have converged if both the distance and speed error are less than 0.01. The convergence times are shown in Table V.

TABLE V: Convergence Time

Controller	Convergence Time (s)
SC	6.630
VGC	4.152
GSC	3.417

While stability is the most important property of a controller, it is useful to have a controller that can perform well in other aspects. As discussed above, a controller that uses minimal effort is desirable in many applications. In Figure 4, the cumulative control effort required to steer the system to some distance from the identity is shown. The SC and GSC are not able to locally optimize as they are tuned for a region.

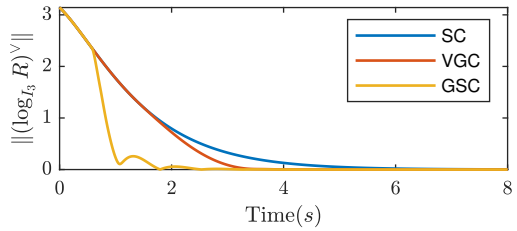

(a) Rotation distance error

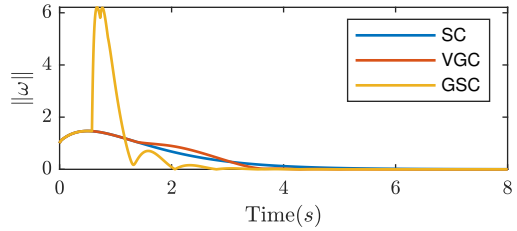

(b) Angular speed error

Fig. 2: The distance and speed error of all three controllers. The static (SC) and varying-gains controller (VGC) have similar behavior while the gain schedule controller (GSC) experiences a sudden change during the first switching phase.

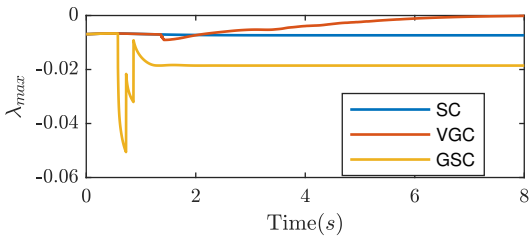

Fig. 3: The maximum eigenvalue of the contraction matrix derived from the contraction condition (4). All controllers maintained a maximum negative eigenvalue, thus all are exponentially stable and satisfy the contraction condition.

Remark 9: The results shows that the GSC convergences 48.46% faster than the SC but requires tremendously (485.06%) more control effort. While the VGC convergences 37.38% faster than the SC, but only uses 10.48% more control effort.

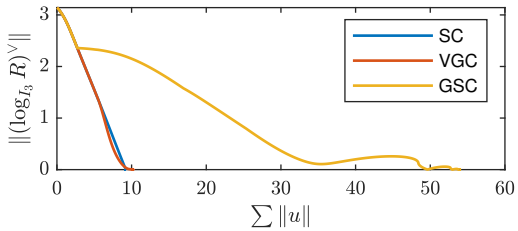

Fig. 4: The cumulative control effort is plotted against the distance error to the identity. The GSC uses comparably more effort to converge than the SC or VGC.

Another desirable controller property is smooth control signals. On real hardware, a discontinuous control may result in unexpected system behavior like motor stalling or

unintended motions that may cause harm. The control signal from the three controllers are shown in Figure 5. The SC and VGC both produce smooth control signals, while the GSC has discontinuities when switching gains.

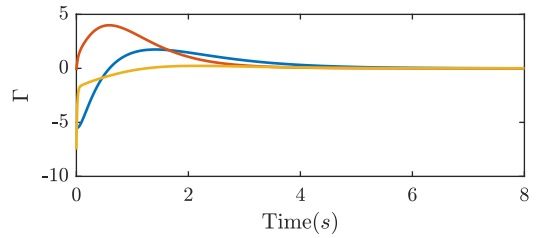

(a) SC Control

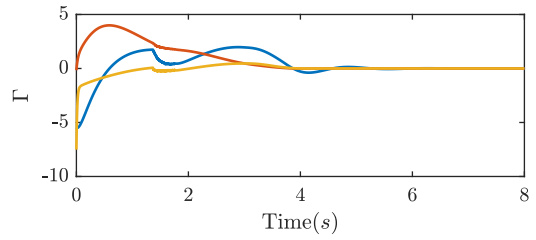

(b) VGC Control

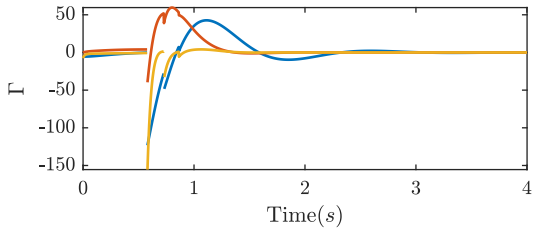

(c) GSC Control

Fig. 5: Control signals from each controller. The SC and VGC produce continuous signals while the GSC has discontinuities. Smoother VGC signals can be obtained by limiting the gain derivative rates in (36).

VI. Conclusion

In this work, a framework was introduced to transform a static gain, feedback, attitude controller to a varying-gains controller via point-wise optimization. An advantage of this formulation is that the new controller leverages the stability results of the static controller to ensure its convergence. The new controller updates the gains online by solving an optimization problem with constraints from Control Barrier and Lyapunov Functions to guarantee stability with optimized, continuous controls. In simulations, the new varying-gains controller converges faster than the static controller using similar control efforts. In addition, the varying-gains controller is smooth with similar convergence times to a discontinuous gain scheduling controller, but requires less control effort.

In future work, we plan to investigate the usage of the point-wise close-form contraction condition (as opposed to the bounds) to increase performance. The challenge is that stability is only guaranteed for a particular state, and the controller is not well-defined when the optimization problem is infeasible.

References

[1] R. Mahony, V. Kumar, and P. Corke, "Multirotor Aerial Vehicles: Modeling, Estimation, and Control of Quadrotor," *IEEE Robotics and Automation Magazine*, vol. 19, no. 3, pp. 20–32, 2012.

[2] M. D. Shuster, "A Survey of Attitude Representations," *Journal of the Astronautical Sciences*, vol. 41, pp. 439–517, Oct. 1993.

[3] D. E. Koditschek, "The application of total energy as a lyapunov function for mechanical control systems," *Contemporary Mathematics*, vol. 97, p. 131, 1989.

[4] F. Bullo and R. M. Murray, "Tracking for fully actuated mechanical systems: a geometric framework," *Automatica*, vol. 35, no. 1, pp. 17–34, 1999.

[5] D. S. Maithripala, J. M. Berg, and W. P. Dayawansa, "Almost-global tracking of simple mechanical systems on a general class of lie groups," *IEEE Transactions on Automatic Control*, vol. 51, no. 2, pp. 216–225, 2006.

[6] T. Lee, M. Leok, and N. H. McClamroch, "Geometric tracking control of a quadrotor uav for extreme maneuverability," *IFAC Proceedings Volumes*, vol. 44, no. 1, pp. 6337 – 6342, 2011.

[7] N. A. Chaturvedi, A. K. Sanyal, and N. H. McClamroch, "Rigid-body attitude control," *IEEE Control Systems Magazine*, vol. 31, no. 3, pp. 30–51, 2011.

[8] K. Sreenath, T. Lee, and V. Kumar, "Geometric control and differential flatness of a quadrotor UAV with a cable-suspended load," *IEEE International Conference on Decision and Control*, vol. 1243000, pp. 2269–2274, 2013.

[9] S. Berkane, A. Abdessameud, and A. Tayebi, "Hybrid global exponential stabilization on SO (3)," *Automatica*, vol. 81, pp. 279–285, 2017.

[10] T. Lee, "Global exponential attitude tracking controls on SO(3)," *IEEE Transactions on Automatic Control*, vol. 60, no. 10, pp. 2837–2842, 2015.

[11] C. G. Mayhew and A. R. Teel, "Hybrid control of rigid-body attitude with synergistic potential functions," in *IEEE American Control Conference*, 2011, pp. 287–292.

[12] ——, "Synergistic potential functions for hybrid control of rigid-body attitude," in *IEEE American Control Conference*, 2011, pp. 875–880.

[13] T. Lee, D. E. Chang, and Y. Eun, "Attitude control strategies overcoming the topological obstruction on SO(3)," in *IEEE American Control Conference*, May 2017, pp. 2225–2230.

[14] B. Vang and R. Tron, "Global attitude control via contraction on manifolds with reference trajectory and optimization," *IEEE International Conference on Decision and Control*, pp. 2006–2013, 2020.

[15] X. Xu, P. Tabuada, J. W. Grizzle, and A. D. Ames, "Robustness of control barrier functions for safety critical control," *IFAC*, vol. 48, no. 27, pp. 54–61, 2015, analysis and Design of Hybrid Systems ADHS.

[16] G. Wu and K. Sreenath, "Safety-critical geometric control for systems on manifolds subject to time-varying constraints," *IEEE Transactions on Automatic Control in review*, 2016.

[17] I. R. Manchester and J. E. Slotine, "Control contraction metrics: Convex and intrinsic criteria for nonlinear feedback design," *IEEE Transactions on Automatic Control*, vol. 62, no. 6, pp. 3046–3053, 2017.

[18] ODROID. Hardkernel co., ltd. [Online]. Available: http://www.hardkernel.com

[19] F. Bullo and A. D. Lewis, *Geometric control of mechanical systems : modeling, analysis, and design for simple mechanical control systems*, ser. Texts in applied mathematics ; 49. New York: Springer, 2005.

[20] W. Lohmiller and J. Slotine, "On contraction analysis for non-linear systems," *Automatica*, vol. 34, no. 6, 1998.

[21] J. W. Simpson-Porco and F. Bullo, "Contraction theory on Riemannian manifolds," *Systems and Control Letters*, vol. 65, no. 1, pp. 74–80, 2014.

[22] B. Vang and R. Tron, "Geometric attitude control via contraction on manifolds with automatic gain selection," *IEEE International Conference on Decision and Control*, pp. 6138–6145, 2019.

[23] R. Tron, "Distributed optimization on manifolds for consensus algorithms and camera network localization," Ph.D. dissertation, John Hopkins University, 2012.

[24] M. Grant and S. Boyd, "CVX: Matlab software for disciplined convex programming, version 2.1," http://cvxr.com/cvx, Mar. 2014.

[25] R. H. Tütüncü, K. C. Toh, and M. J. Todd, "Solving semidefinite-quadratic-linear programs using sdpt3," *MATHEMATICAL PROGRAMMING*, vol. 95, pp. 189–217, 2003.